Connexin 43 as a signaling platform for increasing the volume and spatial distribution of regenerated tissue

Ricardo A. Rosselló[a], Zhuo Wang[b], Eddy Kizana[c], Paul H. Krebsbach[a,b], and David H. Kohn[a,b,1]

Departments of [a]Biomedical Engineering, [b]Biologic and Materials Sciences, University of Michigan, Ann Arbor, MI, 48109-1078 and [c]Department of Cardiology, Johns Hopkins University, Baltimore, MD

Edited by Robert Langer, Massachusetts Institute of Technology, Cambridge, MA, and approved June 12, 2009 (received for review March 15, 2009)

Gap junction intercellular communication (GJIC) is ubiquitous in the majority of vertebrate cells and is required for the proper development of most tissues. The loss of gap junction-mediated cell-to-cell communication leads to compromised development in many tissues and organs. Because cells constantly interact through gap junctions to coordinate tissue functions and homeostasis, we hypothesized that increasing cell-to-cell communication, via genetically engineering cells to overexpress gap junction proteins, could enhance cell differentiation in the interior regions of 3D tissue equivalents, thereby increasing the ability to regenerate larger and more uniform volumes of tissue. To test this hypothesis, we used bone as a model tissue because of the difficulty in achieving spatially uniform bone regeneration in 3D. In bone marrow stromal cells (BMSC), GJIC and osteogenic differentiation were compromised in 3D cultures relative to 2D monolayers and in the core of 3D cultures relative to the surface. Overexpression of connexin 43 (Cx43) via transduction of BMSCs with a lentivirus overcame this problem, enhancing both the magnitude and spatial distribution of GJIC and osteogenic differentiation markers throughout 3D constructs. Transplantation of cells overexpressing Cx43 resulted in an increased volume fraction and spatial uniformity of bone in vivo, relative to nontransduced BMSCs. Increased GJIC also enhanced the effect of a potent osteoinductive agent (BMP-7), suggesting a synergism between the soluble factor and GJIC. These findings present a platform to improve cell-to-cell communication in 3D and to achieve uniformly distributed tissue regeneration in 3D.

bone regeneration | cell–cell communication | gap junctions | virus

Cell-to-cell communication via intercellular chemical and mechanical signals is critical to maintain tissue homeostasis (1). Gap junction intercellular communication (GJIC) is the most direct way of achieving such signaling (2) and is particularly important to maintain synchronized and cooperative behavior of cells in 3-dimensional (3D) tissues (3). Consequently, the absence of gap junctions has been linked with several debilitating diseases and malformations of tissues, such as oculodentaldigital dysplasia, impaired heart function, and certain types of malignant tumors (4, 5). Of the 19 known gap junction subunits, connexin 43 (Cx43) is the most prevalent (6). The ubiquitous nature of this protein throughout most vertebrate cell types makes it a potent signaling platform that enables cells to communicate directly. Cx43 also serves to distribute secondary messengers initiated by other biological cues and stimuli that play a role in cell differentiation and tissue formation, such as bone morphogenetic proteins (BMPs) and parathyroid hormone (PTH) (7). However, characterization of the primary effects of connexins and effects generated by these secondary messengers has mostly involved the in vitro assessment of cells in a 2D monolayer. Such approaches may not reveal the impact of these factors on cell-cell communication in 3D settings in vivo. Limitations in cell-to-cell communication in 3D may hinder the coordinated behavior of cells and inhibit secondary messengers and eventual tissue formation. The governing hypothesis of this investigation, therefore, is that overexpressing Cx43 can be a means to enhance the magnitude and distribution of cell-to-cell communication throughout a 3D environment and can therefore be a powerful strategy in both cell-based regeneration and targeted delivery therapies. This research, therefore, may have a significant impact on tissue regeneration, as well as in developing therapies for diseases characterized by compromised cell-cell communication, such as some cancers and heart disease (8, 9).

In this study, we focused on the effects of Cx43 as a platform to enhance GJIC in 3D, both in vitro and in vivo. Because of the difficulty in producing large and spatially uniform 3D mineralized tissue equivalents (10, 11), bone was used as a model tissue. Such a limitation is, in large part, due to transport constraints and the formation of a peripheral shell of tissue (10, 11). To examine the role of enhanced GJIC in tissue regeneration, we investigated the effects of Cx43 overexpression in bone marrow stromal cells (BMSCs) by transducing these cells with a lentiviral vector encoding the Cx43 gene (LV-Cx43-GFP). Cell-cell communication and osteogenic differentiation of transduced and nontransduced BMSCs were compared in vitro in monolayer (2D) and 3D cultures, and the amount and distribution of bone regenerated was assessed in vivo. Enhancing gap junction function in BMSCs for tissue engineering purposes is attractive because of the stem cell-like properties of these cells (12, 13) that enable them to differentiate into bone (or other tissues), given the proper biological cues (14). To complement the main aims of this study, we also investigated the effects of an osteogenic stimulus, bone morphogenetic protein 7 (BMP-7), coupled with higher GJIC. BMP-7 was chosen because it is a potent osteoinductive agent (15–17) that does not modulate Cx43 expression (18).

Based on our data, we propose that enhanced GJIC in cells genetically engineered to overexpress Cx43 can serve as an approach to spatially distribute cell-cell communication in 3D and achieve larger volumes of more spatially uniform tissue. These results could have a major impact in the design of cell-based tissue engineering strategies and therapies to enhance cell-to-cell communication in 3D tissues.

Results

Characterization of Cx43-GFP Modified BMSCs. Gene transfer efficiency of the GFP-Cx43 fusion gene was 83 ± 4% (Fig. 1*A*) 2 weeks after transduction. Similar efficiency was attained when cells were cotransduced with AD-CMV-BMP7 and LV-Cx43-GFP (85 ± 5%) and in control cells with only LV-GFP (87 ± 7%). An increase in Cx43 secretion occurred when cells were transduced with LV-Cx43-GFP. The total expression of Cx43 in BMSCs transduced with LV-Cx43-GFP was significantly higher (3.74- ± 0.49-fold increase; $P < 0.001$ vs. both groups) compared to nontransduced BMSCs (1.0 ± 0.29) and LV-GFP transduced controls (0.89 ± 0.11) (Fig. 1*B*).

Author contributions: R.A.R., E.K., P.H.K., and D.H.K. designed research; R.A.R. and Z.W. performed research; E.K. contributed new reagents/analytic tools; R.A.R., P.H.K., and D.H.K. analyzed data; and R.A.R. wrote the paper.

The authors declare no conflict of interest.

This article is a PNAS Direct Submission.

[1]To whom correspondence should be addressed. E-mail: dhkohn@umich.edu.

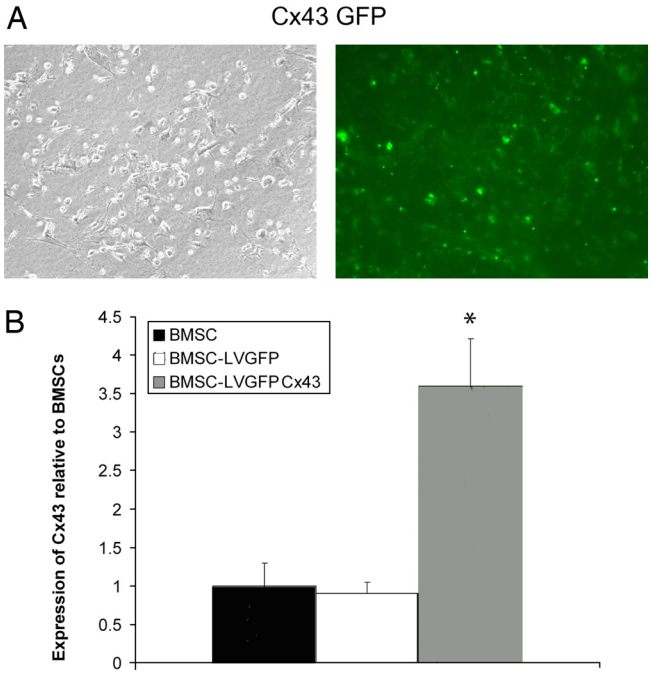

Fig. 1. BMSCs transduced with LV-Cx43-GFP. Expression of the Cx43-GFP (*A*) in transduced BMSCs under phase contrast and fluorescent microscopy indicates that a high percentage of cells express the Cx43-GFP fusion gene. Quantification of Western blot band intensities showed a significant increase (3.74- ± 0.49-fold increase; $P < 0.001$) in Cx43 expression in cells that were transduced compared to nontransduced BMSCs and BMSCs transduced with GFP only (*B*). * indicates $P < 0.001$ versus BMSC and BMSC-LV-GFP control groups.

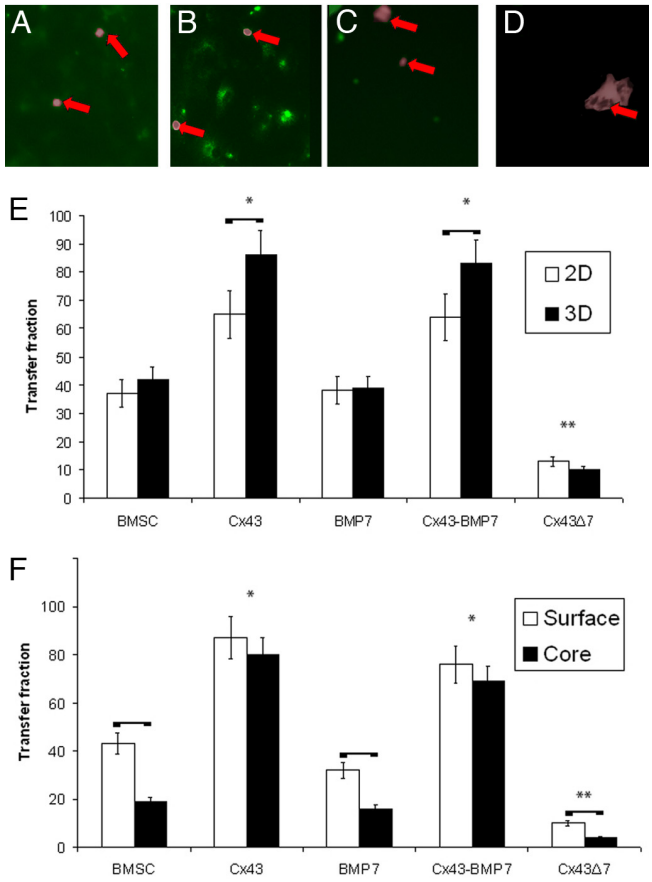

Fig. 2. GJIC in BMSCs is enhanced with Cx43 overexpression. Images demonstrate the transfer of calcein in BMSCs (*A*), BMSC-Cx43 (*B*), BMSC-BMP7 (*C*), and mutant BMSC-Cx43Δ7 cells (*D*) after 5 h of exposure to donor cells. Arrows indicate donor cells (DiI, wide field inverted) overlaid in the images. The transfer fraction of calcein-AM was measured for cells cultured in monolayer and 3D (*E*). Cells overexpressing Cx43 had a significantly higher transfer fraction than non-Cx43-transduced cells. Transfer was significantly enhanced in 3D when cells overexpressed Cx43 relative to 2D. Cells that did not overexpress Cx43 showed significantly less dye transfer in the core of the scaffolds compared to the periphery, whereas no significant difference was evident in cells overexpressing Cx43 (*F*). Horizontal bars represent pairs that are significantly different; * indicates groups that are significantly greater than BMSCs; ** indicates groups that are significantly less.

Overexpression of Cx43 Increases GJIC. BMSCs transduced with Cx43 exhibited significantly higher transfer of calcein than non-transduced BMSCs, both in cells cultured in 2D and 3D (Fig. 2; $P < 0.001$ for both Cx43 and Cx43-BMP-7 vs. BMSC and BMP-7). There was no significant difference in transfer fraction between Cx43 and Cx43-BMP7 treated cells or between BMSCs and BMP-7 transduced BMSCs, suggesting that BMP-7 does not modulate GJIC. Cells transduced with the Cx43 gene mutant exhibited significantly less dye transfer than both BMSCs and BMSCs transduced to overexpress Cx43 ($P < 0.001$). Taken together, the dye transfer data suggest that inhibition or overexpression of Cx43 leads to hindered or amplified GJIC, respectively. When cells overexpressed Cx43, the percentage of cells that internalized calcein in 3D cultures was significantly greater than the percentage of cells that internalized the dye in 2D cultures (Fig. 2*E*; $P < 0.001$ for both Cx43 and Cx43-BMP7 vs. BMSC and BMP-7). BMSCs and BMSCs transduced with BMP-7 showed no significant difference in transfer fraction between 2D and 3D cultures. Cells transduced with control and empty vectors did not demonstrate a significant difference in transfer fraction versus BMSCs. BMSCs and BMSCs transduced with BMP-7 or Cx43Δ7 exhibited significantly less calcein transfer in the core of the scaffolds relative to the periphery [Fig. 2*F*; P (BMSCs) < 0.002, P (BMP-7) < 0.001, P (Cx43Δ7) < 0.013]. However, in cells overexpressing Cx43, there was no statistical difference in transfer fraction between the surface and core sections of the scaffolds (Fig. 2*F*).

Overexpression of Cx43 Enhances Magnitude and Spatial Distribution of Osteogenic Differentiation Markers. Increased Cx43 expression in BMSCs was associated with significantly higher levels of osteocalcin (OCN) mRNA relative to controls (Fig. 3*A*). Two days after differentiation was induced, cells overexpressing Cx43 and Cx43-BMP7 exhibited significantly higher levels of OCN ($P < 0.001$ vs. all other groups). Cells overexpressing BMP-7 only expressed higher levels of OCN than BMSCs ($P < 0.023$), but the expression level was significantly less than in cells overexpressing Cx43 ($P < 0.001$). Similar trends were observed on day 8, although OCN expression increased 4–5× compared to day 2 in cells overexpressing Cx43. At day 16, cells overexpressing both Cx43 and BMP-7 produced significantly more OCN ($P < 0.001$ vs. all other groups). Cells overexpressing Cx43Δ7 expressed significantly less OCN than all other cells ($P < 0.001$, against all other cells at all times). Control vectors showed no significant difference in OCN mRNA expression compared to BMSCs.

Significant differences in osteogenic differentiation also existed between 2D and 3D cultures (Fig. 3*B*). OCN expression was significantly greater in 2D cultures compared to 3D cultures of BMSCs ($P < 0.021$), BMSCs overexpressing BMP-7 ($P < 0.001$), and empty vector controls. When cells overexpressed Cx43, there were no significant differences in OCN expression between the 2D and 3D cultures, implying that cell-cell communication may be an essential mechanism underlying the differences in differentiation between 2D and 3D cultures. Both BMSCs and BMSC-BMP7 expressed significantly higher levels of OCN on the surface relative

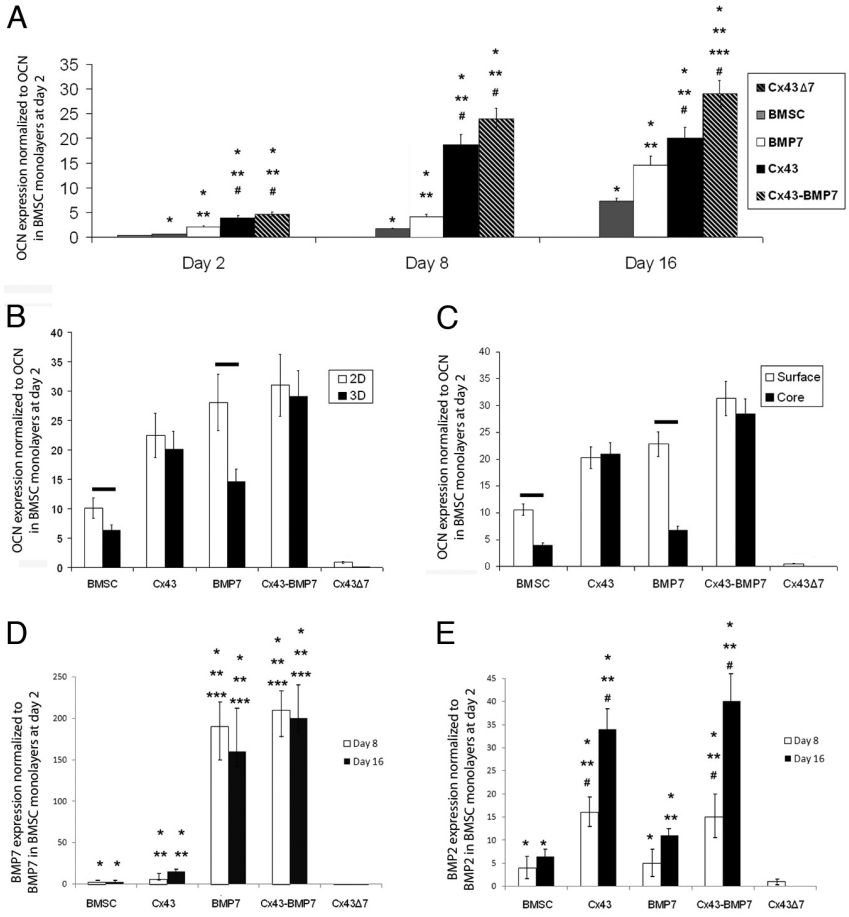

Fig. 3. Cx43 overexpression is associated with higher levels of OCN mRNA expression (*A*), suggesting that increased GJIC results in an enhanced capacity of cells to undergo osteogenic differentiation. Increased cell-cell communication also increases the production of osteoinductive soluble factors (*D* and *E*). Overexpression of Cx43 also had significant effects on OCN expression when comparing 2D to 3D cultures (*B*). OCN mRNA expression was significantly greater in 2D for cells that did not overexpress Cx43, while cells that overexpressed Cx43 exhibited no significant difference in level of OCN expression between 2D and 3D cultures. Analysis of the surface versus core of the scaffolds (*C*) suggests that increased GJIC in the interior regions of a tissue equivalent can enhance the magnitude and reduce spatial gradients in differentiation. Significant increases are indicated by * versus Cx43Δ7, ** vs. BMSC, *** vs. Cx43, # vs. BMP-7. Horizontal bars indicate pairs that are significantly different.

to the core of the scaffolds (Fig. 3*C*, $P < 0.001$ for both). Furthermore, the effect of BMP-7 was significantly neutralized in 3D, with a 4-fold decrease in OCN expression relative to monolayer culture and a nonsignificant increase over BMSCs in 3D ($P < 0.092$). When both Cx43 and BMP-7 were overexpressed, the differences between 2D and 3D were no longer present.

Cells overexpressing Cx43 also produced significantly higher levels of mRNA for the soluble osteoinductive factors BMP-7 and BMP-2 than nontransduced BMSCs (Fig. 3*D* and *E*; $P < 0.001$ at both day 8 and 16). Cells overexpressing BMP-7 exhibited a 100- to 200-fold increase in BMP-7 relative to BMSCs and expressed significantly higher levels than BMSC-Cx43 cells ($P < 0.001$ for all times). However, cells overexpressing Cx43 expressed significantly higher levels of BMP-2, than cells overexpressing BMP-7 [P (day 8) $= 0.05$, P (day 16) < 0.001].

Cx43 Gene-Modified Cells Regenerated More Bone in Vivo. Bone regenerated by BMSCs (Fig. 4*A–C*), BMSCs overexpressing Cx43 (Fig. 4*D–F*), and BMSCs overexpressing BMP-7 (Fig. 4*G–I*) all exhibited a cortical-like shell with an enclosed marrow cavity. However, bone formed from Cx43 transduced cells exhibited a thicker cortex and a smaller amount of marrow. Ossicles formed from cells cotransduced with Cx43 and BMP-7 exhibited larger amounts of trabecular-like bone (Fig. 4*J–L*). The volume fraction of bone in ossicles produced by transplanted BMSC-Cx43 cells was significantly greater than the volume fraction in ossicles formed from BMSCs at all time points [Fig. 4*M*; P (4 wks) < 0.032, P (8 wks) < 0.001, P (12 wks) < 0.003]. Transplantation of cotransduced cells led to significantly higher bone volume fractions (BVF) than all other groups at 8 and 12 weeks ($P < 0.001$ against all groups at both times). After 12 weeks, cells in ossicles formed via the overexpression of Cx43 still exhibited high levels of GFP expression (Fig. 4*N–P*), indicating the continued expression of Cx43 in a large percentage of cells in vivo.

Cortical thickness was significantly greater in ossicles formed from Cx43 transduced BMSCs (Fig. 5*B*) compared to nontransduced BMSCs ($P < 0.001$ at all times). Ossicles formed by cotransduced BMSCs exhibited thicker cortical-like bone compared to ossicles formed by BMSCs and BMP-7 ($P < 0.001$, at 4 and 12 weeks). There was no statistical difference in cortical thickness of bone formed by cotransduced cells versus cells overexpressing Cx43. After 4 weeks of transplantation, the BMSC-Cx43 group had significantly more trabecular-like bone than the BMSC group ($P < 0.001$). These differences were not observed at 8 weeks ($P < 0.56$), but were again significant at 12 weeks ($P < 0.001$). The trabecular-like BVF was significantly higher in ossicles formed from cotransduced cells after 8 and 12 weeks of implantation (Fig. 5*C*).

Discussion

The data presented in this paper demonstrate that Cx43 overexpression can be a means to enhance the magnitude and spatial distribution of cell-cell communication in 3D and as a strategy to regenerate tissue in vivo. Specifically, we showed that cells expressing higher levels of Cx43 exhibit higher GJIC (Fig. 2), greater osteogenic differentiation in vitro (Fig. 3), and when transplanted, form tissue of larger volume (Fig. 4) and more uniform spatial distribution (by generating larger amounts of trabecular bone in the interior of tissue equivalents) (Fig. 5). Using Cx43 as a signaling platform may therefore have beneficial effects in both cell-based tissue engineering and targeted gene therapy.

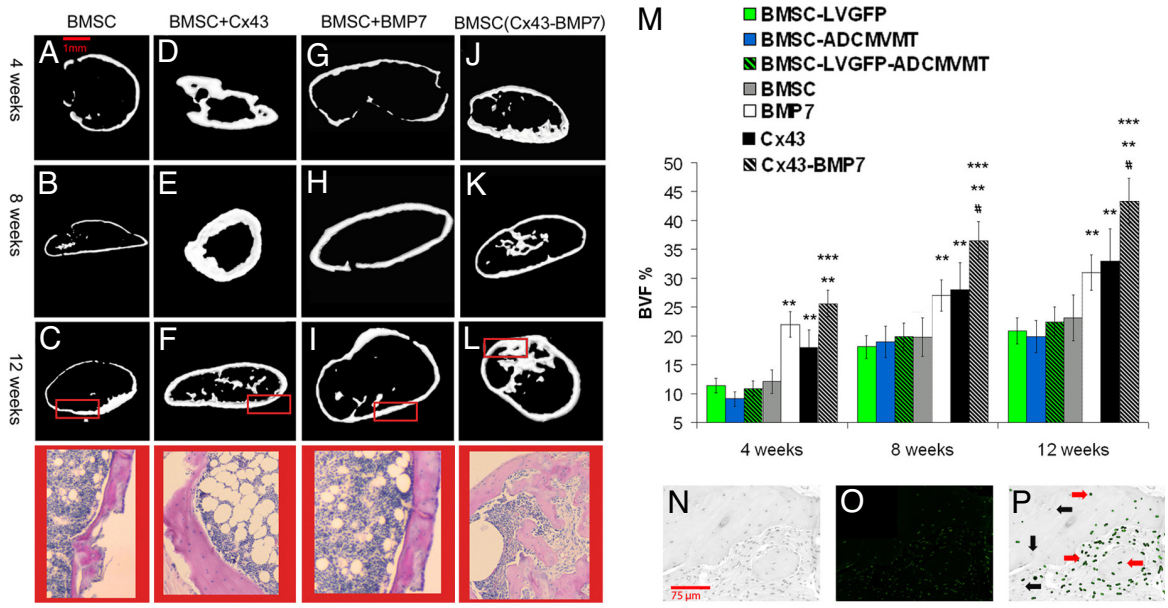

Fig. 4. MicroCT renderings and histological sections (taken from regions of microCT images highlighted by red rectangle) of bone regenerated following transplantation of BMSCs (*A–L*). Different patterns of bone regeneration between BMSCs and BMSCs overexpressing Cx43 are observed. BVF quantifies these differences (*M*). Cells transduced with Cx43 and cotransduced with BMP-7 form larger volumes of tissue compared to BMSCs. Contrast image (*N*), image of GFP fluorescence (*O*), and co-localized image (*P*) of the same section of tissue regenerated 12 weeks after transplantation of BMSCs overexpressing Cx43. The continued extent of the GFP-Cx43 fusion gene expression is observed. Significant increases are indicated by ** vs. BMSC, *** vs. Cx43, # vs. BMP-7.

Increased bone regeneration in the core of 3D tissue equivalents was also achieved (Fig. 5), suggesting an essential role for GJIC in tissue regeneration. Regeneration of large and spatially uniform volumes of tissue has been elusive. When seeded into a 3D extracellular matrix analog, cells in the periphery thrive and differentiate, while those in the core of the scaffold are less viable and exhibit compromised differentiation (10, 11). This limitation leads to incomplete regeneration over the volume of a 3D template, making it less clinically relevant (19–21). Our findings therefore suggest that enhanced GJIC enables cues to distribute more effectively, and cells, when induced by endogenous means, can differentiate and regenerate greater quantities of functional tissue. Some of the specific cues that have been linked with bone differentiation and turnover and are small enough to permeate through Cx43 generated gap junctions are calcium (Ca^{2+}), inositol triphosphate (IP3), and ATP (1).

Extrapolating data generated from 2D monolayers into more practical 3D analogs is a challenging problem in tissue engineering. While some tissues can be approximated by a monolayer (e.g., skin), most others are more complex in their hierarchy and 3D nature (e.g., bone). To gain insight into the ability of increased GJIC to enhance the spatial distribution of cells capable of appropriate differentiation, we cultured cells in monolayer (2D) and in scaffolds (3D) and assessed differences in GJIC and osteogenic differentiation between 2D and 3D cultures and between the surface and inner regions of scaffolds. Cells overexpressing Cx43 exhibited higher GJIC in 3D culture relative to 2D, whereas control cells and cells overexpressing only BMP-7 experienced similar levels of GJIC in 2D and 3D (Fig. 2*E*). Cells overexpressing Cx43 also exhibited similar levels of OCN expression in 2D and 3D cultures, in contrast to decreased levels of OCN mRNA in BMSCs and BMSCs overexpressing only BMP-7 in 3D cultures compared to a monolayer (Fig. 3*B*). Taken together, these findngs point to a greater significance of GJIC in cells seeded in 3D constructs compared to 2D monolayer and suggest that more gap junction channels are formed when cells are cultured in 3D, likely because of the larger number of cell-cell surface contacts in 3D compared to 2D.

Further insights into the impact that GJIC has in 3D cultures is derived by comparing the core sections of 3D cell-scaffold constructs to surface sections (Figs. 2*F* and 3*C*). Cells that do not overexpress Cx43 exhibit significantly less GJIC and expression of osteogenic differentiation markers in the core of the 3D cultures. In contrast, cells overexpressing Cx43 do not exhibit significant differences in GJIC and differentiation between the core and surface, suggesting that enhanced GJIC enables a more uniform spatial distribution of differentiation cues in 3D.

Overexpression of Cx43 also led to increases in soluble osteoinductive factors (Fig. 3*D* and *E*), suggesting that enhanced osteogenic differentiation by cells overexpressing Cx43 can occur through indirect as well as direct effects of Cx43. The significant increase in cell-cell communication resulting from the overexpression of Cx43 (Fig. 2) is due to channel formation resulting from the direct action of Cx43. It is the activity of Cx43 and not just its structural presence that is critical, because the deletion mutant that has the same structure and docking ability but does not result in channel formation inhibits cell-cell communication and leads to only low levels of differentiation and bone formation. Following transplantation, cells continue to overexpress Cx43 and are capable of forming viable channels with other transplanted and/or host cells (Fig. 4*P*), implying that the in vivo response to Cx43 is, at least in part, a direct effect of increased GJIC. The indirect effect of Cx43 is exhibited by the increased expression of soluble factors that regulate differentiation and bone formation.

The in vitro results demonstrate an enhancement in osteogenic differentiation with elevated Cx43 expression. However, an in vivo assessment of bone formation is a more robust proof of principle. In vivo, transplantation of cells overexpressing Cx43 resulted in a larger quantity of bone relative to controls (Fig. 4). Bone regenerated from cells exhibiting enhanced GJIC also exhibited a thicker cortex and larger amount of trabecular-like bone, as characterized by more porous bone in the core of the ossicles (Fig. 5). Although the in vitro data suggest that Cx43 has a more potent effect on osteogenic differentiation than BMP-7, the in vivo data demonstrate that the volume fraction of bone is not significantly different between ossicles formed from BMSC-Cx43 versus BMSC-BMP7

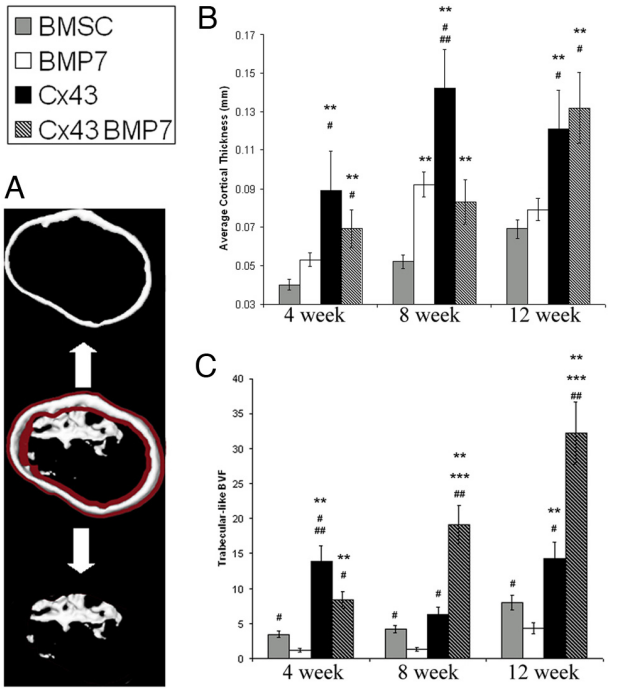

Fig. 5. Cortical-like bone thickness and trabecular-like bone volume fraction of tissue engineered bone (*A*). Cx43-transduced cells produced an average cortical thickness that was significantly greater than the cortical thickness of bone produced by BMSCs (*B*). The trabecular-like BVF (*C*) was also significantly greater in bone regenerated from cells overexpressing Cx43 compared to BMSCs at 4 and 12 weeks. Cotransduced cells led to a significantly larger fraction of trabecular-like bone at 8 and 12 weeks compared to all other groups. Significant increases are indicated by ** vs. BMSCs, *** vs. Cx43, # vs. BMP-7, and ## vs. Cx43-BMP7.

cells. However, the spatial patterns of bone growth are distinct (Figs. 4 and 5). The bone developed from BMSC-BMP7 cells rapidly forms a peripheral shell that restricts bone formation in the interior of the scaffold. Therefore BMP-7 results in a limited amount of trabecular bone formation and a less favorable spatial distribution of tissue (Fig. 5C). This in vivo data parallels the 3D in vitro data showing that BMP-7 overexpression results in limited differentiation in the interior regions of the scaffolds. Cx43 overexpression does not induce a larger amount of bone formation, but leads to bone formation that is more evenly distributed within the volume of the scaffold (Figs. 4 and 5). This suggests that the higher level of cell-cell connectivity created by the connexin channels enables bone formation to occur in the core sections of the 3D construct as well as at the periphery. The reason why the bone volume fractions are similar between the Cx43 and BMP-7 cases is because of the heterotopic bone formation that occurs with BMP-7, in which the ossicles formed from BMSC-BMP7 cells extend beyond the boundaries of the scaffold. Overall, the in vivo data suggests that the higher level of cell-to-cell communication enables cells to act in a more synchronized manner, allowing full development of tissue throughout a scaffold.

GJIC can also distribute signals arising from a secondary stimulus to neighboring cells (22). To test the effect of higher GJIC in tandem with another stimulus, cells were also induced to overexpress BMP-7. This growth factor was chosen because it has potent osteoinductive effects, but does not modulate the expression of Cx43 (18). Enhanced GJIC increased the osteogenic effect of BMP-7, suggesting that the overexpression of Cx43 synergistically enhances the effects of other stimuli, perhaps by enhancing the distributed differentiation potential of cells in 3D, an outcome observed both in vitro (Fig. 3) and in vivo (Figs. 4 and 5). The experiments with BMP-7 represent a strategy that could potentially be extended to other tissues by using Cx43 with other growth factors or stimuli that enhance the regeneration of a tissue of interest.

Our findings suggest that increasing GJIC via overexpression of Cx43 can be a powerful tool to overcome limitations inherent in cell-cell communication and regeneration of tissue in 3D. This approach can also complement the effect of a secondary stimulus, leading to regeneration of larger and more uniform volumes of tissue. This strategy may be applied to a range of cells and tissues with the aim of controlling tissue development in 3D. Ultimately, our approach of controlling cell-to-cell communication may overcome the longstanding problem of inducing synchronized cell behavior in 3D cultures and developing clinically meaningful tissue equivalents.

Materials and Methods

Viral Vector Production. Vectors encoding Cx43 and BMP-7 were produced by the University of Michigan Vector Core. The development and production of the lentiviral vector encoding Cx43-GFP (LV-Cx43-GFP) has been described (23). The vector system was based on the HIV-1 virus, and the plasmids required for vector production were kindly supplied by Professor Inder Verma from the Salk Institute, San Diego, CA. The development and production of the adenoviral vector encoding BMP-7 under the transcriptional control of the human CMV promoter has also been described (15). Empty vectors devoid of a transgene and vectors encoding GFP were also produced for lentivirus (LV-MT, LV-GFP) and adenovirus (Ad-CMV-MT) and used as controls. A construct containing a 7-bp deletion mutant (LV-Cx43Δ7) that produces connexin structures but is disabled from engaging in GJIC was used as a negative control.

Culture and Transduction of BMSCs. Bone marrow stromal cells were isolated from the long bones of 5-week-old C57BL/6 mice (University of Michigan UCUCA approval #08633), as described (24). BMSCs mixed with α-MEM (Gibco Laboratories) enriched with 10% FBS (Gibco Laboratories) and 100 μg/mL penicillin G plus 100 IU/mL streptomycin were plated at 30,000 cells/cm^2 at 37 °C in 5% CO_2. Cells were passaged 2 times before transduction. For LV-Cx43-GFP, LV-GFP, and LV-MT transductions, lentiviral vectors with a titer of 10^6 transducing U/mL were used on day 3–4 of subculture. Protamine sulfate (8 μg/mL) was used to enhance transduction efficiency. Five milliliters filtered vector-enriched α-MEM was added to the cultures for 16 h (transduction phase), followed by replacement with fresh media for 6–8 h (recovery phase). The cells were exposed to 3 cycles of transduction. After 14 days of incubation, transduced BMSCs were examined under fluorescent microscopy to determine transduction efficiency via GFP fluorescence. Ten random fields per well were photographed, and transduction was measured as the average fraction of fluorescent cells relative to total cells in the field. Transductions with ADCMVBMP7 and ADCMVMT were performed as described (16) to achieve a multiplicity of infection of 200 plaque forming units (PFU).

Western Blot Analysis. Western blots were performed using mouse anti-Cx43 with GAPDH as a control. Cells were lysed in lysis buffer (66 mM Tris-HCl, 5 mM EDTA, 5 mM EGTA, 10 mM Na-phosphate, 5 mM NaF, 5 mM Na_3VO_4, 2.5 mM PMSF, 10 mM NEM, 2% SDS, 0.5% Triton X-100, pH 8.0). Protein extraction was performed on cell lysates from BMSCs and BMSCs overexpressing Cx43. Cell suspensions were centrifuged, the supernatant was discarded, and cell pellets were resuspended in water and lysed by sonication. Protein concentration was determined using the Bradford method (Bio-Rad Laboratories). Fifty micrograms total protein from each group was resuspended in 1× buffer, separated on 8% SDS/PAGE and transferred to nitrocellulose sheets. Nonspecific protein binding was blocked by incubation of nitrocellulose sheets. Blots were incubated in 1% nonfat dry milk solution in PBS overnight with gentle shaking, washed 3 times with PBS, and incubated with primary antibodies for 2.5 h. The resulting bands were quantified by densitometry (ImageQuant; GE Healthcare). To quantify the total Cx43 expression in Cx43-GFP transduced cells, the 74-kDa band (sum of Cx43 and GFP fusion protein) was analyzed. The results are reported as the following ratio: [(Cx43 level in BMSC-Cx43/GAPDH level in BMSC-Cx43)/(Cx43 level in BMSC/GAPDH level in BMSC)]. Experiments were performed in triplicate and were done 1 week after the end of transduction. One-way ANOVA was performed on the band intensities to determine whether Cx43 secretion was significantly different ($P < 0.05$) between groups.

2D and 3D Cell Cultures. Equivalent cell densities were used in the 2D and 3D experiments to allow for effects of Cx43 to be compared between 2D and 3D microenvironments. Cells (2.5×10^6) were seeded into each $3 \times 3 \times 3$ mm^3 gelfoam construct. Gelfoam (Amersham Pharmacia and Upjohn) is a water-

insoluble, nonelastic, porous material prepared from purified porcine skin gelatin and water, whose specifications were determined elsewhere (25). The constructs had a surface area of 460 cm^2/g and a porosity of 98%. Cell seeding efficiency was 99%. Seeding density was estimated from the surface area and weight of the scaffolds (0.058 g). Total surface area was $\approx$25 cm^2, yielding an average density of 100,000 cells/cm^2. In 2D experiments, cells were seeded at high densities to achieve 100,000 cells/cm^2 and cultured on polystyrene in MEM-α with 10% FBS, 100 mg/mL penicillin G, and 100 IU/mL streptomycin. Studies that examined peripheral versus core GJIC and differentiation were performed by placing 2 sponges in 96-well plates, 1 on top of the other. The thickness of the top and bottom sponges was 0.5 and 2.5 mm, respectively. Cell-gelatin constructs were press-fit into the wells. The bottom sponge was the core section of the scaffold, as the walls of the well blocked flux from the bottom or sides. All sponges were prewet in α-MEM. Cells (2.5 million) were collected, suspended in 50 μL medium, and loaded onto each sponge by capillary action. Both 2D and 3D cultures were induced to differentiate with osteogenic medium [88% MEM-α, 9% FBS, 100 mg/mL penicillin G and 100 IU/mL streptomycin, 1% 100$\times$ β-glycerophosphate (0.216 g/mL), 1% 100$\times$ L-ascorbic acid-phosphate (5 mg/mL), 0.05% 5,000$\times$ dexamethasone (0.28 mg/mL)] 7 days after the start of culturing. Cells were cultured in 2D and 3D for 2, 8, or 16 days after induction of differentiation.

Dye Transfer Experiments. Fluorescent dye transfer was used to assess GJIC. Calcein-AM (10 μm, gap junction-permeable; Molecular Probes) and Vybrant-DiI (membrane tracker; Molecular Probes) were used to label donor cells grown to confluence in 12-well plates. As a negative control, 50 μM gap junction uncoupler α-glyccirrhetinic acid (AGA) was used (Sigma). Donor cells were added to potential recipient cells at a ratio of 1:8 once recipient cells were confluent in 2D or 3D (n = 6/cell type for both 2D and 3D). After 5 h, cells were harvested for quantification of GJIC by flow cytometry (FaCSCalibur; BD Biosciences) and visualization by inverted fluorescent microscopy. A 2-way ANOVA was used to determine significant differences in percent of calcein-positive recipient cells between cell types and between 2D and 3Ds. Two-tailed t-tests were used to determine significant differences between cells in the surface versus core of scaffolds.

Real-Time PCR Analysis. Real-Time PCR was used to detect the expression of osteocalcin (OCN), BMP-2, and BMP-7. PCR was performed using an ABI Prism 7700 sequence detection system (Applied Biosystems). Primers and TaqMan probes were designed using Primer Express design software (ABI; Applied Biosystems). The primer sequences were: OCN, forward 5′-CCAGCGACTCTGAGTCTGACAA-3′, and reverse 5′-CCGGAGTCTATTCACCACCTTACT-3′. BMP-7 and BMP-2 were probed using TaqMan gene expression assays [ABI, Assay ID: (BMP7), Mm00432101_m1; (BMP2), Mm01340178_m1; Applied Biosystems). Cells differentiated for 2, 8, or 16 days and total RNA was extracted (TRIzol; Invitrogen), purified (RNeasy; Qiagen), and treated with DNase I. PCR conditions were: 50 °C for 2 min and 95 °C for 10 min, followed by 50 cycles of 95 °C for 15 s and 60 °C for 1 min. No-template controls were run for each primer set, and 18s rRNA (ABI) endogenous controls were run for each sample. mRNA expression levels for each sample were normalized to endogenous rRNA 18s levels and expression levels of genes of interest at the onset of differentiation. All reactions were performed in quintuplet. Two 1-way ANOVAs were used to determine significant differences in mRNA levels of OCN, BMP-7, and BMP-2 versus cell type and dimension (2D versus 3D). Differences in OCN expression between cells in the surface and core were assessed with a 2-tailed t-test.

In Vivo Transplantation. Surgery was performed in nude mice (nu/nu) by transplanting gelatin scaffolds ($3 \times 3 \times 3$ mm^3) seeded with 2×10^6 cells (University of Michigan UCUCA approval no. 08633). Cells were seeded as described for the 3D in vitro cultures. Mice were anesthetized by an i.p. injection of 1 mg/10 g ketamine and 0.1 mg/10 g xylazine. A 3-cm longitudinal incision was made overlaying the spine. Four s.c. pockets were made using blunt dissection through the s.c. tissue. In each pocket, 1 of the cell-gelatin specimens (BMSC, BMSC-Cx43, BMSC-BMP7, BMSC-Cx43-BMP7, BMSC-LVMT, BMSC-AD-CMV-MT) or an acellular gelatin specimen (randomly assigned) was implanted and closed with wound clips or sutures. Four, 8, and 12 weeks after transplantation, mice were euthanized and regenerated ossicles were extracted and stored in 70% ethanol until further analysis.

MicroCT Image Acquisition and Analysis. Bone ossicles were scanned on a high-resolution cone beam microCT system (Enhanced Vision Systems) The X-ray source voltage and current were 80 kVp and 80 μA, respectively. Projection images were acquired over 198 ° using 2×2 binning and an exposure time of 1100 ms followed by correction and reconstruction using the Feldkamp cone-beam algorithm to create 3D images with an isotropic voxel size of 18 μm (26). Bone volume fractions (BVF) were determined via a MatLab program (The MathWorks) that integrated all grayscale voxels above a threshold of 1,100. The program traced the perimeter of each 2D slice and integrated the perimeters of all slices to determine the 3D surface area. The number of voxels inside the surface defined the total volume. A custom program was written to differentiate the trabecular and cortical bone. Using the 2D microCT sections, the centroid was calculated with a MatLab script (27) and used as a frame of reference to divide the ossicles into regions. Cortical bone was defined as the continuous bone formation in the periphery of the ossicle. The program calculated this thickness by averaging the thickness at 10 ° increments from the geometric center of the ossicle. Trabecular BVF was the remaining bone fraction normalized to the potential trabecular space (total bone volume - cortical bone volume).

Histology and Morphological Analyses. A subset of the regenerated bone ossicles (2 per group $\times$ 6 groups) were harvested, rinsed in water, decalcified in 10% formic acid for 5 days, and embedded in paraffin. Thin 5-μm sections were cut and placed on 10 slides with 3 sections per slide. The tissue was deparaffinized, hydrated, and the first, fifth, and tenth slides were left unstained to observe GFP expression or stained with H&E. Image Pro Plus 4.0 was used to image the histological sections to observe bone formation, cortical thickness, and trabecular-like bone formation.

ACKNOWLEDGMENTS. We thank Michael Mayer and Martin Philbert for their helpful comments. This work was supported by National Institutes of Health Grants R01 DE 015411, DE 013380, and P30-AR46024.

1. Jorgensen NR, et al. (2003) Activation of L-type calcium channels is required for Gap junction-mediated intercellular calcium signaling in osteoblastic cells. *J Biol Chem* 278:4082–4086.
2. Cotrina ML, et al. (1998) Connexins regulate calcium signaling by controlling ATP release. *Proc Natl Acad Sci USA* 95:15735–15740.
3. Jongsma HJ, Wilders R (2000) Gap junctions in cardiovascular disease. *Circ Res* 86:1193–1197.
4. Flenniken AM, et al. (2005) A Gja1 missense mutation in a mouse model of oculodentodigital dysplasia. *Development* 132:4375–4386.
5. King TJ, Bertram JS (2005) Connexins as targets for cancer chemoprevention and chemotherapy. *Biochim Biophys Acta* 1719:146–160.
6. Saez JC, Berthoud VM, Branes MC, Martinez AD, Beyer EC (2003) Plasma membrane channels formed by connexins: Their regulation and functions. *Physiol Rev* 83:1359–1400.
7. Civitelli R, et al. (1998) Regulation of connexin43 expression and function by prostaglandin E2 (PGE2) and parathyroid hormone (PTH) in osteoblastic cells. *J Cell Biochem* 68:8–21.
8. Huang R, et al. (2002) Connexin 43 suppresses human glioblastoma cell growth by down-regulation of monocyte chemotactic protein 1, as discovered using protein array technology. *Cancer Res* 62:2806–2812.
9. Lai A, et al. (2006) Oculodentodigital dysplasia connexin43 mutations result in non-functional connexin hemichannels and gap junctions in C6 glioma cells. *J Cell Sci* 119:532–541.
10. Holy CE, Shoichet MS, Davies JE (2000) Engineering three-dimensional bone tissue in vitro using biodegradable scaffolds: Investigating initial cell-seeding density and culture period. *J Biomed Mater Res* 51:376–382.
11. Ishaug SL, et al. (1997) Bone formation by three-dimensional stromal osteoblast culture in biodegradable polymer scaffolds. *J Biomed Mater Res* 36:17–28.
12. Dorshkind K, Green L, Godwin A, Fletcher WH (1993) Connexin-43-type gap junctions mediate communication between bone marrow stromal cells. *Blood* 82:38–45.
13. Bianco P, Robey PG (2001) Stem cells in tissue engineering. *Nature* 414:118–121.
14. Krebsbach PH, Kuznetsov SA, Bianco P, Robey PG (1999) Bone marrow stromal cells: characterization and clinical application. *Crit Rev Oral Biol Med* 10:165–181.
15. Franceschi RT, Wang D, Krebsbach PH, Rutherford RB (2000) Gene therapy for bone formation: In vitro and in vivo osteogenic activity of an adenovirus expressing BMP7. *J Cell Biochem* 78:476–486.
16. Krebsbach PH, Gu K, Franceschi RT, Rutherford RB (2000) Gene therapy-directed osteogenesis: BMP-7-transduced human fibroblasts form bone in vivo. *Hum Gene Ther* 11:1201–1210.
17. Rutherford RB, et al. (2002) Bone morphogenetic protein-transduced human fibroblasts convert to osteoblasts and form bone in vivo. *Tissue Eng* 8:441–452.
18. Chatterjee B, et al. (2003) BMP regulation of the mouse connexin43 promoter in osteoblastic cells and embryos. *Cell Commun Adhes* 10:37–50.
19. Amiel C, Bailly C, Friedlander G (1987) Multiple hormonal control of the thick ascending limb functions. *Adv Nephrol Necker Hosp* 16:125–136.
20. Beaman FD, Bancroft LW, Peterson JJ, Kransdorf MJ (2006) Bone graft materials and synthetic substitutes. *Radiol Clin North Am* 44:451–461.
21. Langer R, Vacanti JP (1993) Tissue engineering. *Science* 260:920–926.
22. Stains JP, Lecanda F, Screen J, Towler DA, Civitelli R (2003) Gap junctional communication modulates gene transcription by altering the recruitment of Sp1 and Sp3 to connexin-response elements in osteoblast promoters. *J Biol Chem* 278:24377–24387.
23. Dull T, et al. (1998) A third-generation lentivirus vector with a conditional packaging system. *J Virol* 72:8463–8471.
24. Leonova EV, Pennington KE, Krebsbach PH, Kohn DH (2006) Substrate mineralization stimulates focal adhesion contact redistribution and cell motility of bone marrow stromal cells. *J Biomed Mater Res A* 79:263–270.
25. Liu X, Smith LA, Hu J, Ma PX (2009) Biomimetic nanofibrous gelatin/apatite composite scaffolds for bone tissue engineering. *Biomaterials* 30:2252–2258.
26. Feldkamp LA, Goldstein SA, Parfitt AM, Jesion G, Kleerekoper M (1989) The direct examination of three-dimensional bone architecture in vitro by computed tomography. *J Bone Miner Res* 4:3–11.
27. Wallace JM, et al. (2006) The mechanical phenotype of biglycan-deficient mice is bone- and gender-specific. *Bone* 39:106–116.